Supplementary Information

pH and Basicity of Ligands Control the Binding of Metal-ions to *B.cereus* B1 β-Lactamase

Hasina Motara, Dharmit Mistry, David R. Brown, Robert A. Cryan, Michaël Nigen and Michael I. Page

1. Sequential binding model with the formation of both EM and EM_2.

Formation of the mononuclear enzyme EM and the binuclear enzyme EM_2 occurs in two sequential steps. At equilibrium, the fractions of the enzyme species existing as E, EM and EM_2 are functions of the two binding constants K_{b1} and K_{b2} and the concentrations of E, M and EM. The sequential binding of metal-ions is represented by **Scheme 1** and the association constant K_{b1} is given by the quadratic **eqn. 1** and K_{b2} is given by a similar equation.

$$\mathbf{E + M = EM} \quad K_{b1} \qquad\qquad \mathbf{EM + M = EM_2} \quad K_{b2}$$

Scheme 1

$$K_{b1}[EM]^2 - K_{b1}[E]_i[EM] - K_{b1}[M]_i[EM] - [EM] + K_{b1}[E]_i[M]_i = 0 \qquad \textbf{eqn.1}$$

The initial concentrations of enzyme in the analyte solution in the calorimetric cell is (E_i) and that the volume of the cell is V_o. The metal ion concentration in the titrant solution is (M_i). The titration is carried out in defined steps, in which a fixed volume of titrant (ΔV) is added at each step and the heat released or absorbed is measured after each injection of titrant into the sample cell. The object is to predict the concentration of EM and EM_2 produced in the cell with each injection. From this, with suitable values for ΔH for the two reactions, the heat against added titrant profile is calculated. Values for the two binding constants and for the two enthalpies are assumed (tried) and are used in the model to predict the differential heat output in an ITC experiment as a function of added metal titrant solution.

The equilibrium constant (K_{b1}), which determines the equilibrium concentration of EM produced after the first injection, is defined by **eqn.1**, and K_{b2} is defined similarly for the second equilibrium determining the concentration of EM_2. In the model, the two equations for K_{b1} and K_{b2} (**Scheme 1**) are treated separately to obtain the concentrations of EM and EM_2 formed.

For a single injection of metal-ion into the cell containing the enzyme, the model is used first to calculate the equilibrium concentration of EM, and hence the concentrations of M and E remaining in solution, *assuming that only reaction 1 occurs*, by solving the quadratic eqn. 1 (the correct root is self-evident). Using the equilibrium concentrations of EM and M arising from this first calculation, the equilibrium conditions for reaction 2 are then applied and the concentration of EM_2 calculated, plus new values for the concentrations of EM and M. Using the resultant concentrations of E, M, EM and EM_2, the sequence of calculations for equilibrium concentrations from the two reactions are repeated in an iterative process, refining the equilibrium values for the concentrations of EM and EM_2, until changes in concentration become negligibly small. In our programme, these equilibrium concentrations are inserted back into the equilibrium constant expressions to ensure self-consistency.

For subsequent injections the initial concentrations of E and M are calculated from the remaining concentrations of enzyme and metal in the cell after the previous injection. The increases in [EM] and [EM_2] are calculated as before, and this is repeated for each injection of titrant. These changes in concentrations of EM and EM_2 as the titration proceeds are converted to a heat output, firstly by converting to changes in numbers of moles in the cell, and then by using values of the molar enthalpies of reaction, ΔH_1 and ΔH_2, chosen for the model.

A practical consideration has to be taken into account in the model as in the ITC experiment, the cell is first completely filled with analyte solution (1.4194 cm^3). When titrant is added (injected to the bottom of the cell so mixing is very rapid) the cell overflows, and the solution that overflows does not contribute to the measured heat. This means that assumptions have to be made about the extent to which the full heat of reaction is measured. We assume that on each injection, equilibrium becomes established in the overall volume of V_o + ΔV, and all the heat released from this volume is captured. This is reasonable if the rate of reaction and the rate of heat release/capture are fast relative to the rate of injection of the titrant. The time constant of the calorimeter is very small so this is almost certainly so. The other assumption is that only solution which remains in the cell (V_o) is available for reaction when the next injection is made, and that the solution that has overflowed has been lost. Also, the components in the cell are diluted with each injection relative to the previous injection and a dilution factor is applied each time (**eqn. 2**).

$$D_{fM} = \frac{\Delta V}{V_0 + \Delta V} \qquad \textbf{eqn.2}$$

The moles of EM formed (ΔN_{EM}) after the first injection is given by **eqn. 3** where [EM] is the concentration of EM after the injection, V_0 is the active cell volume (V_0 = 1.4194 cm^3) and ΔV is the injection volume.

$$\Delta N_{EM} = [EM]_1 (V_0 + \Delta V) \qquad \textbf{eqn.3}$$

For injections beyond the first (eg the ***ith***) of metal, the moles of EM ($\Delta N_{EM\,i}$) formed can be calculated using **eqn. 4.**

$$\Delta N_{EMi} = [EM]_i (V_0 + \Delta V) - ([EM]_{i-1} V_0)$$ **eqn.4**

The moles of EM_2 formed (ΔN_{EM2}) on each injection is calculated in the same way. The differential heat (Q) in terms of kcal mol^{-1} of metal ion injectant for any injection ***i*** is calculated using **eqn.5** where ΔH_1 and ΔH_2 are the molar enthalpies of reactions 1 and 2 respectively, ΔV is the injection volume for each injection into the cell and M_i is the initial metal concentration in the syringe.

$$Q_{totali} = \frac{\left(\frac{\Delta N_{EMi} * \Delta H1}{1000} + \frac{\Delta N_{EM2i} * \Delta H2}{1000}\right)}{\Delta V * M_i}$$ **eqn. 5**

The differential heat, Q_i, can be divided between that associated with EM formation and that associated with EM_2 formation (**eqn.6**), and the overall heat output for the ***i***th injection, Q_{Total}***i*** is of course the sum of the two which is then converted to a differential heat with respect to the added metal-ion.

2. 'Concerted', positive cooperative binding model without the formation of the mononuclear species EM.

The binding equilibrium constant (K_b) (**Scheme 2**) is given by **eqn.6** and the concentration of EM_2 produced after the

$$E + 2\,M \underset{}{\overset{K_b}{\rightleftharpoons}} EM_2$$ **Scheme 2**

$$K_b = \frac{[EM_2]}{[E][M]^2}$$ **eqn.6**

the first injection is defined by **eqn. 7** with the initial concentrations of enzyme $[E]_i$ and metal-ion $[M]_i$. The initial concentration of the enzyme (E_i) is that in the analyte solution in the calorimetric cell and that of the metal-ion (M_i) is that added from the titrant solution.

$$K_b = \frac{[EM_2]}{([E]_i - [EM_2])([M]_i - 2\,[EM_2])^2}$$ **eqn. 7**

Both binding sites are filled even when there is less than 1 equivalent of metal-ion to the enzyme, so that the only species present are E and EM_2. For subsequent injections the concentration of E and M are calculated from the remaining concentrations of enzyme and metal in the cell, this equation is a cubic in terms of $[EM_2]$ (**eqn. 8**).

$$-(4K_b)[EM_2]^3 + 4K_b([E]_i + [M]_i)[EM_2]^2 - (4K_b[E]_i[M]_i + K_b[M]_i^2 + 1)[EM_2] + K_b[E]_i[M]_i^2 = 0$$ **eqn.8**

The roots (**eqn. 9**) of the eqn.11 for the concentration of EM_2 for each injection are solved analytically using Derive 6.

$$Root_1 = \frac{E_i + M_i}{3} - \frac{\sqrt{P}\cos\left(\frac{\cos^{-1}\left(-\frac{N\sqrt{P}}{O}\right)}{3}\right)}{3}$$

$$Root_2 = \frac{E_i + M_i}{3} + \frac{\sqrt{P}\sin\left(\frac{\sin^{-1}\left(\frac{N\sqrt{P}}{O}\right)}{3} + \frac{\pi}{3}\right)}{3}$$

$$Root_3 = \frac{E_i + M_i}{3} - \frac{\sqrt{P}\sin\left(\frac{\sin^{-1}\left(\frac{N\sqrt{P}}{O}\right)}{3}\right)}{3}$$

eqn. 9

Where:

$$N = K_b\left(8\,[E]_i^3 K_b - 12\,[E]_i^2[M]_i K_b + 3\,[E]_i\left(2\,[M]_i^2 K_b - 3\right)[M]_i\left([M]_i^2 K_b + 9\right)\right)$$

$$O = \left(4\,[E]_i^2 K_b - 4\,[E]_i[M]_i K_b + [M]_i^2 K_b - 3\right)^2$$

$$P = \left(\frac{4\,[E]_i^{\,2}K_b - 4[E]_i[M]_iK_b + [M]_i^{\,2}K_b\, -\, 3}{K_b}\right)$$

The cubic expression has three roots, but the root which has a physical meaning is obtained using a branched statement as the correct root for EM_2 lies between 0 and $M_i/2$ and cannot be greater than the initial concentration of enzyme and metal for a given injection. The dilution effects (**eqn.2**) are incorporated and the differential heats/kcal/mole of injectant are calculated using **eqn.10** with respect to EM_2.

$$Q_i = \frac{\left(\frac{\Delta N_{EM2i} \,*\, \Delta H}{1000}\right)}{\Delta V \,*\, M_i} \qquad \textbf{eqn.10}$$

Titration curves of different binding constants were simulated with initial enzyme (E_i) and metal (M_i) concentrations of 1.8 x 10^{-5} M and 3.6 x 10^{-4} M, respectively, and a metal increment volume (ΔV) of 1.0 x 10^{-5} l (**Figure 1**).

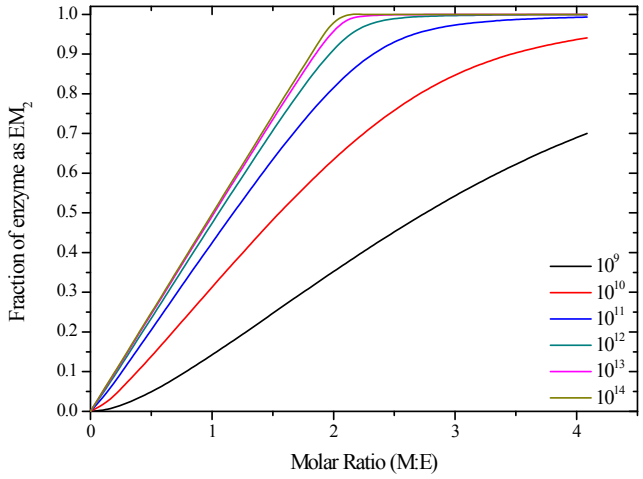

Figure 1 Simulated fraction of enzyme bound to metal-ion as EM_2 as a function of molar ratio (metal added/enzyme) at different binding constants $K_b = 10^9$ to 10^{14} M^{-2}.

Figure 1 shows how the binding constant alters the fraction of enzyme bound to metal-ion as a function of molar ratio (M:E). At a high binding constant 10^{12} to 10^{14} M^{-2} the fraction of enzyme bound to the metal as EM_2 is near completion with a slope of 0.50 as a function the molar ratio (M:E). The enzyme is fully saturated as EM_2 at a molar ratio of about 2 for binding constants of 10^{14} and 10^{13} M^{-2}, but a binding constant of 10^{12} M^{-2} requires a little more metal-ion with 99% saturation occurring at 2.5 molar equivalents. Reducing the binding constant to 10^{10} M^{-2} starts to show an initial downward curvature at low metal:enzyme ratio even with this apparently 'high' binding constant complete saturation (> 99%) requires more than 4 molar equivalents of metal-ion. A binding constant of 10^9 M^{-2} shows a definite sigmoidal shape graph with an increasing concave line until a molar ratio of 1 after which the fraction of EM_2 becomes linear up until a molar ratio of 2. Even after 4 molar equivalents of metal-ion have been added, only 70% of the enzyme exists as EM_2 . Some examples of the fraction of enzyme bound to the metal as EM_2 as a function of the molar ratio (M:E) and various binding constants are given in **Table 1**.

K_b	% EM_2 1:1 (M:E) molar ratio	2:1(M:E) molar ratio
10^{14}	49	97
10^{13}	48	95
10^{12}	47	90
10^{11}	42	81
10^{10}	31	63
10^9	14	35

Table 1 Percentage of the enzyme existing as EM_2 at different binding constants at molar ratios (M:E) of 1:1 and 2:1.

The data in Figure 1 can be transformed to differential heats per mole of injectant using an enthalpy ΔH = 10.0 kcal mol^{-1} per mole of product EM_2 formed (**Figure 2**). As two moles of metal-ion are required for each mole of EM_2 formed, 5.0 kcal mol^{-1} is the maximum heat released per mole of metal-ion injectant if all the metal complexed with the enzyme to form EM_2. This is shown with a binding constant of 10^{14} M^{-2} even at molar ratios of less than 2:1. A binding constant of 10^{13} M^{-2}

shows initially, at low M:E ratio, the enthalpy of binding is lower than the maximum, compatible with less than full conversion of the added metal-ion to EM_2, but as the molar ratio M:E increases the differential heats per mole of injectant reaches the maximum. If the binding constant is decreased further this increase, at low M:E ratios, in the initial differential binding enthalpy becomes more pronounced but does not reach the maximum - shown clearly even by binding constants of 10^{12} and 10^{11} M^{-2}. As the molar ratio M:E increases above about 1.5, the differential heats per mole of injectant then decrease, as normal, as a decreasing fraction of enzyme is converted to EM_2 with increasing added metal-ion as equilibrium is approached. With binding constants less than 10^{10} M^{-2}, the profiles cease to be 'normal' titration curves.

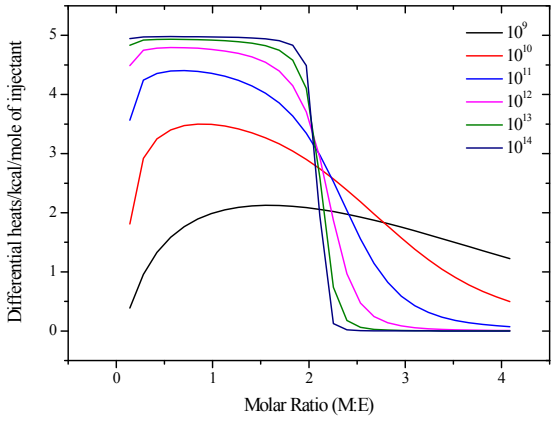

Figure 2 Simulation of the differential heats per kcal per mole of injectant metal-ion as a function of molar ratio (M:E) at different binding constants for 'concerted' formation of binuclear EM_2.

3. Comparison of the sequential and concerted models

The sequential and concerted models were compared using various binding constant ratios (K_{b2}/K_{b1}) termed α (**eqn. 11**). The fraction of enzyme existing as either EM or EM_2 and the sum of both species ($EM+EM_2$), θ, (**eqn.12**) were plotted against molar ratio (M:E) as a function of variable binding constant ratios $\alpha = 10^4, 10^3, 10^2, 10, 1, 10^{-1}$ and 10^{-2}.

$$\alpha = \frac{K_{b2}}{K_{b1}} \qquad \textbf{eqn. 11} \qquad\qquad \theta = \frac{[EM] + [EM_2]}{E_i} \qquad \textbf{eqn.12}$$

The resulting plots of the fraction of enzyme bound as EM and EM_2 can then be converted to differential heat outputs using any values of ΔH. Shown here are ΔH values of 5.0 kcal mol^{-1} for both EM and EM_2 in the sequential binding model as these are more likely to show apparent single binding events in the ITC output. **Figures 3-9** show simulated plots using an initial enzyme concentration (E_i) in the cell (1.4194 ml) and of 1.8 x 10^{-5} M and injecting 1.0 x 10^{-5} l of titrant metal-ion concentration of 3.6 x 10^{-4} M for a total of 29 injections. For comparison, equivalent plots are shown for the 'concerted' binding event simulating $E + 2M \rightleftharpoons EM_2$ using the same heat (i.e.ΔH = 10.0 kcal mol^{-1} for the overall reaction). In **Figures 3-7** for the sequential model $K_{b1} = 10^5$ M^{-1} and K_{b2} is altered to achieve different values of α. An α value of 10^4 (**Figure 3**) shows, in the sequential model, that the fraction of EM (black line) present is negligible compared to the fraction of enzyme bound as EM_2 (red line). The maximum enthalpy of 5.0 kcal mol^{-1} is produced initially during the titration as all of the metal-ion added is converted to EM_2 without significant formation of EM. Both the fraction of enzyme present as EM_2 and the resulting heat output are superimposable with the concerted binding model assuming 'direct' formation to EM_2. At α = 10^3 (**Figure 4**), a similar fraction of EM_2 is formed in both models, with again negligible concentrations of EM in the sequential scheme, and the total heat per mole of product is the theoretical maximum of 5.0 kcal mol^{-1}.
When α is reduced to 100 (**Figure 5**) differences between the concerted and sequential models are discernible. For the latter, at a molar ratio of 1:1 (M:E), 5% EM (black line) and 45% EM_2 (red line) are formed; at 2:1 (M:E) there is 3% EM and 88% EM_2. The concerted model (magenta line) gives, at molar ratios of 1:1 and 2:1 (M:E), 47% and 91% of the enzyme is present as EM_2, respectively. Conversion to EM_2 in the sequential model (red line) is lower than that in the concerted model but in addition there is significant EM produced even up to a molar ratio of almost 3:1. Consequently, the total fraction of enzyme converted to metallo-enzyme species θ at a fixed molar ratio (M:E) is greater in the sequential than in the concerted model. A striking feature of the differential enthalpies plot is that in both models, the differential heat is less than the maximum at the beginning of the titration which shows up as a 'kink' in the plot, presumably because at very low metal-ion concentrations not all of the metal-ion is converted to metallo-enzyme species .
When α = 10 (**Figure 6**), there is a large difference between two models - the sequential model predicts relatively high EM concentrations of 14% and 11%, at molar ratios of 1:1 and 2:1 (M:E), respectively. The percentages of EM_2, at molar ratios 1:1 and 2:1 (M:E) respectively, in the sequential model are 35, 74 and 42 and 81% in the concerted model. The total fraction of enzyme converted to metallo-enzyme, θ, at a fixed M:E ratio is greater in the sequential than in the concerted model.

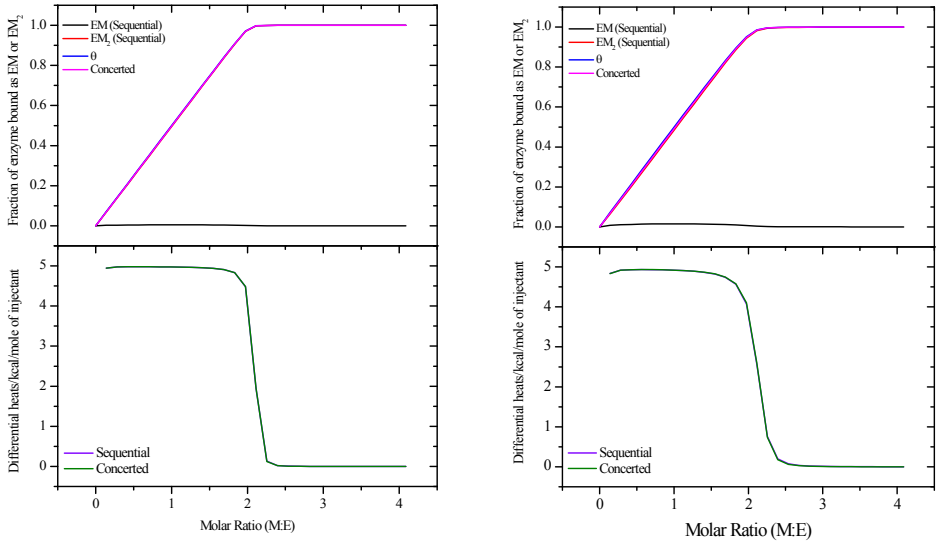

Figures 3 and **4.** Fraction of EM (—), EM_2 (—) and θ (—) as a function of molar ratio (M:E) for the sequential binding model using $K_{b1} = 10^5$ M^{-1} and, left, $K_{b2} = 10^9$ M^{-1} ($\alpha = 10^4$) and, right, $K_{b2} = 10^8$ M^{-1} ($\alpha = 10^3$), are indistinguishable from the concerted model (—) using, left, $K_b = 10^{14}$ M^{-2} and ,right, $K_b = 10^{13}$ M^{-2}. The bottom graph shows the differential heats kcal.mole^{-1} of injectant metal-ion against molar ratio (M:E) for the sequential (—) and concerted (—) models.

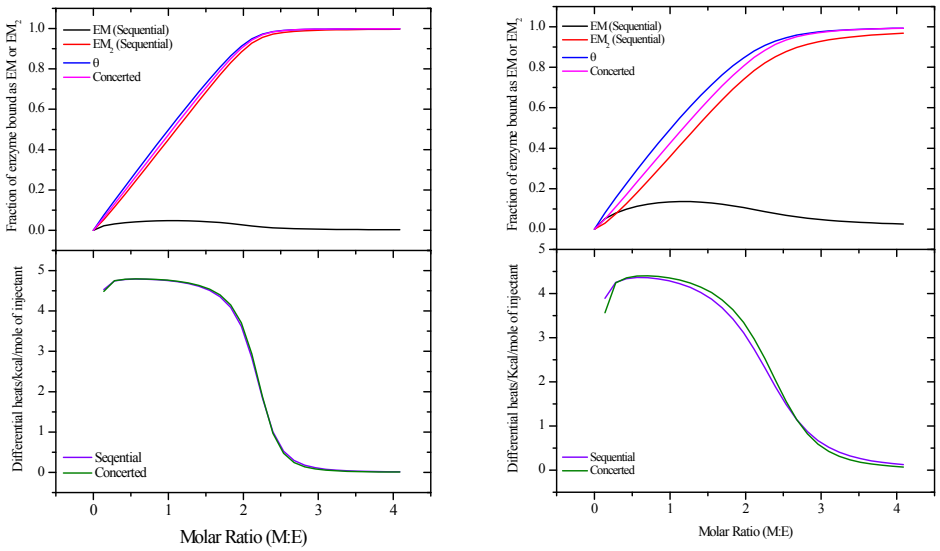

Figures 5 and **6.** Fraction of EM (—), EM_2 (—) and θ (—) as a function of molar ratio (M:E) for the sequential binding model using $K_{b1} = 10^5$ M^{-1} and, left, $K_{b2} = 10^7$ M^{-1} ($\alpha = 10^2$) and, right, $K_{b2} = 10^6$ M^{-1} ($\alpha = 10$), the concerted model (—) using, left, $K_b = 10^{12}$ M^{-2} and ,right, $K_b = 10^{11}$ M^{-2}. The bottom graph shows the differential heats kcal.mole^{-1} of injectant metal-ion against molar ratio (M:E) for the sequential (—) and concerted (—) models.

A α = 1, (**Figure 7**) $K_{b1} = K_{b2} = 10^5$ M^{-1}, both EM and EM_2 are produced in the sequential model at least up to molar ratios (M:E) of 4:1. At low metal-ion concentrations the fraction of EM_2 in the sequential process (red line) shows a 'concave' dependence up to a molar ratio (M:E) of 1.5:1, where the fraction of EM reaches a maximum (33%). At a molar ratio of 2:1 (M:E) 32% of the enzyme exists as EM, 44% as EM_2 and 24% still unbound, free E. With an overall binding constant $K_{b1}.K_{b2}$ (10^{10} M^{-2}) saturation requires a ratio M:E > 4:1. The concerted model shows a significantly different profile compared to the sequential model with 31% of the enzyme present as EM_2 at M:E = 1:1 and at 2:1 63%. This difference between the two models is then reflected in the differential heats.

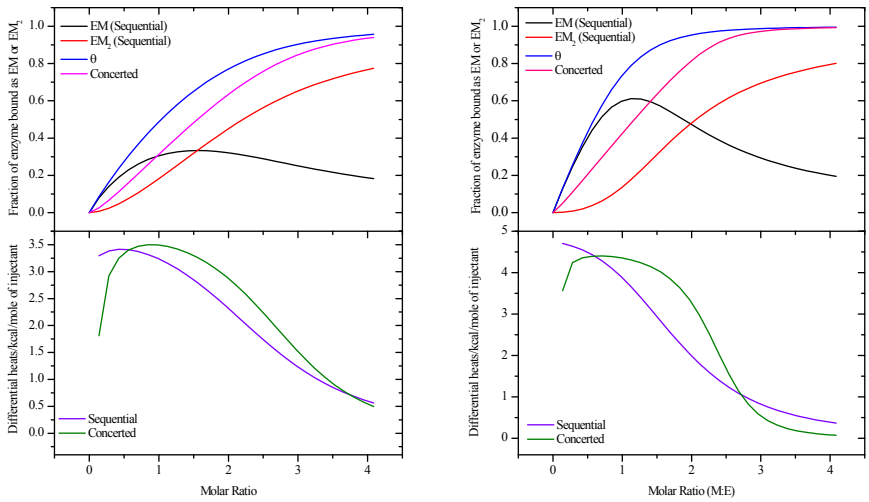

Figures 7 and 8. Fraction of EM (—), EM_2 (—) and θ (—) as a function of molar ratio (M:E) for the sequential binding model using, left, $K_{b1} = 10^5$ M^{-1} and $K_{b2} = 10^5$ M^{-1} (α = 1) and, right, $K_{b1} = 10^6$ M^{-1} $K_{b2} = 10^5$ M^{-1} (α = 10^{-1}), the concerted model (—) using, left, $K_b = 10^{10}$ M^{-2} and, right, $K_b = 10^{11}$ M^{-2}. The bottom graph shows the differential heats kcal.mole^{-1} of injectant metal-ion against molar ratio (M:E) for the sequential (—) and concerted (—) models.

At α = 0.1(**Figure 8**) at a molar ratio of 1:1 (M:E) 60% of the enzyme exists as EM and 13% as EM_2 in the sequential model compared to 42% EM_2 in the concerted model. At a M:E ratio of 2:1 in the sequential model 48% and 47% of the enzyme exists as EM and EM_2, respectively, whereas in the concerted model there is 81% EM_2. The overall fraction of enzyme converted to metallo-enzyme species θ, in the sequential model is higher than that of the fraction existing as EM_2 in the concerted model. A single binding event is produced when the enthalpy of the two binding sites are the same or very similar even when $K_{b1} > K_{b2}$.

When α = 0.01(**Figure 9**) $K_{b1} = 10^8$ M^{-1} and $K_{b2} = 10^6$ M^{-1} the formation of the mononuclear complex is the dominant species at a molar ratio of 1:1 (M:E) with 83% in the form of EM and only 7% as EM_2; only when the M:E ratio is > 1, is the fraction of EM_2 significant in the sequential model. At a ratio of 2:1 (M:E) 22% of the enzyme exists as EM and 78% as EM_2 in the sequential model. As shown previously, the concerted model with $K_b = 10^{14}$ M^{-2} predicts a total conversion of metal-ion to EM_2 even at molar ratios (M:E) below 1. The overall fraction of the enzyme that has reacted, (θ, $(EM+EM_2/E_i)$) in the sequential model is greater than the fraction of enzyme as EM_2 in the concerted model at all molar ratios. A single binding event is produced when the enthalpy of the two binding site are the same or very similar although $K_{b1} > K_{b2}$.

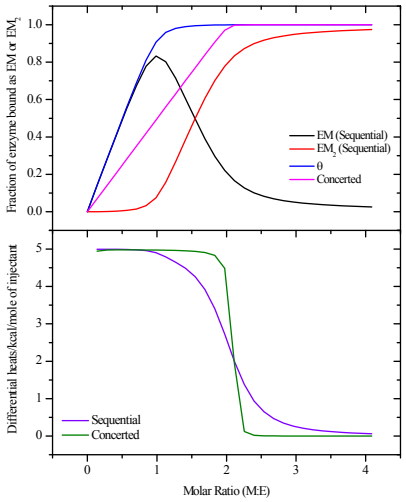

Figure 9. Fraction of EM (—), EM_2 (—) and θ (—) as a function of molar ratio (M:E) for the sequential binding model using $K_{b1} = 10^8$ M^{-1} and $K_{b2} = 10^6$ M^{-1} (α = 10^{-2}), the concerted model (—) using $K_b = 10^{14}$ M^{-2}. The bottom graph shows the differential heats kcal.mole^{-1} of injectant metal-ion against molar ratio (M:E) for the sequential (—) and concerted (—) models.

4. Comparison of differential heat isotherms with different enthalpies and binding constants and using the sequential model.

The shape of the differential heat isotherms varies significantly using different enthalpies for the two steps at constant α values using the sequential model. As shown before, when α = 1 ($K_{b1} = K_{b2} = 10^6$ M^{-1}) and $\Delta H_1 = \Delta H_2 = 5.0$ kcal mol^{-1} a 'normal' titration curve is observed, albeit with an apparent single event. However, when ΔH_2 is varied from 5.0 to 1.0 kcal mol^{-1} the differential heat is less than the maximum at the beginning of the titration at low molar ratios M:E which shows up as a 'kink' in the plot, an upwards concave response is produced with increasing M:E (**Figure 10**) - ΔH_1 is having a greater effect than ΔH_2 on the overall profile. When ΔH_1 is decreased with ΔH_2 kept constant = 5.0 kcal mol^{-1}, the enthalpy starts off at the given ΔH_1 value, which gradually increases which decreases again as metal-ion is added.

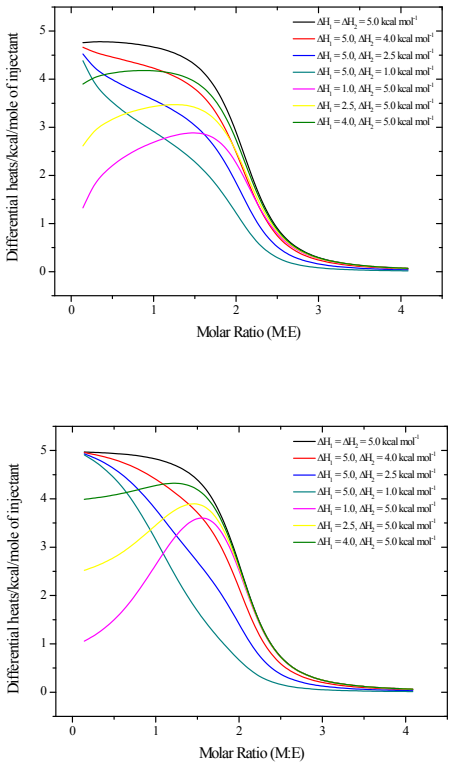

Figures 10 and 11 $K_{b1} = K_{b2} = 10^6$ M^{-1} (α = 1), left, and $K_{b1} = 10^7$ M^{-1} and $K_{b2} = 10^6$ M^{-1} (α = 0.1), right,at different ΔH_1 and ΔH_2 values, shown as differential heats per kcal per mole of injectant against molar ratio (M:E).

When α = 0.1 with $K_{b1} = 10^7$ M^{-1} and $K_{b2} = 10^6$ M^{-1} (**Figure 11**) and ΔH_1 is greater than ΔH_2, a similar effect is seen in the differential heats per kcal per mole of injectant plots against the ratio M:E. When $\Delta H_1 = 5.0$ kcal mol^{-1} and $\Delta H_2 = 2.5$ kcal mol^{-1} the difference of 2.5 kcal mol^{-1} is discernible as a 'bump' in the plot at a molar ratio of about 1.75, indicative of a two step process. This is less profound when there is a difference between ΔH_1 and ΔH_2 of 4.0 kcal mol^{-1}. When $\Delta H_1 < \Delta H_2$, the enthalpy increases with increasing M:E., reaches a maximum then decreases as all the enzyme in the cell becomes saturated.

When α = 0.02, K_{b1} is 50 times greater than K_{b2} (**Figure 12**), when $\Delta H_2 = 5.0$ kcal mol^{-1} and ΔH_1 is decreased, the plots are similar to Figure 11. When $\Delta H_1 = 5.0$ kcal mol^{-1} and ΔH_2 is decreased the indication of a two step process becomes more pronounced and is clearly seen with a difference of 1.0 kcal mol^{-1} ($\Delta H_1 = 5.0$ kcal mol^{-1} and ΔH_2 =4.0 kcal mol^{-1}) and is even more apparent with a larger difference between the two ΔH values.

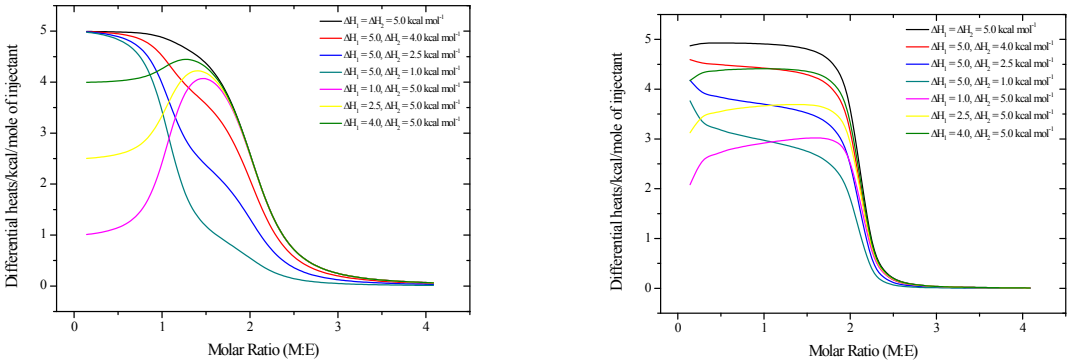

Figure 12 and 13 K_{b1} = 5 x 10^7 M^{-1} and K_{b2} = 10^6 M^{-1} (α = 0.02), left, and K_{b1} = 10^6 M^{-1} and K_{b2} = 10^7 M^{-1} (α = 10), right, at different ΔH_1 and ΔH_2 values, shown as differential heats per kcal per mole of injectant against molar ratio (M:E).

When $K_{b2} > K_{b1}$ (α = 10 and 50) and $\Delta H_1 = \Delta H_2$ = 5.0 kcal mol^{-1}, a single binding event is observed. When α = 10 (**Figure 14**) and ΔH_1 is constant at 5.0 kcal mol^{-1} and ΔH_2 is decreased, similar to when α = 1, an upwards concave response is produced with increasing M:E. When ΔH_2 = 5.0 kcal mol^{-1} is constant and ΔH_1 is decreased, a sharp concave downwards 'kink' is observed initially up to approximately a molar ratio (M:E) of 0.5 which gradually increases due to the larger ΔH_2 which then diminishes as the enzyme becomes saturated. If the binding constant is increased by 5 fold (**Figure 15)**, ΔH_1 has a slightly larger contribution to the profile as the initial 'kink' up to a molar ratio of 0.5 is less than when K_{b1} = 10^6 M^{-1} and K_{b2} = 10^7 M^{-1} (Figure 14).

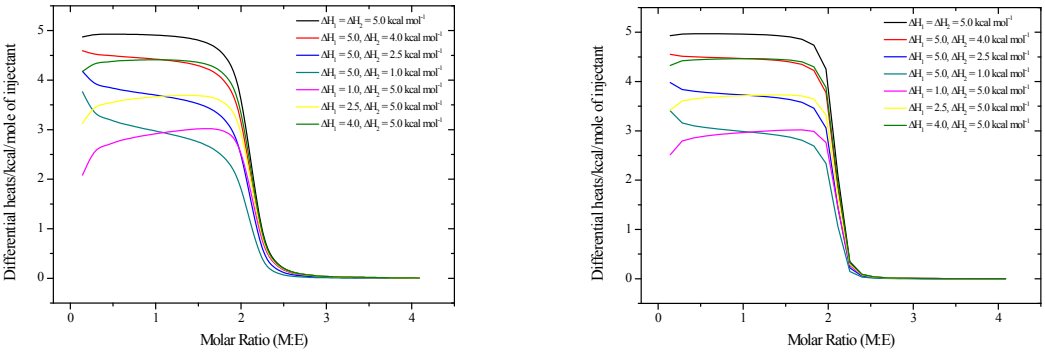

Figures14 and 15 K_{b1} = 10^6 M^{-1} and K_{b2} = 10^7 M^{-1} (α = 10), left, and K_{b1} = 10^6 M^{-1} and K_{b2} = 5 x 10^7 M^{-1} (α = 50) , right, at different ΔH_1 and ΔH_2 values, shown as differential heats per kcal per mole of injectant against molar ratio (M:E).

SI Table 1 Summary of N and observed enthalpy change data for **zinc** ion solution titrated into apoBcII solution as function of pH and buffer type at 25^0C.

		pH					
Buffers		**5.20**	**5.60**	**6.00**	**6.35**	**6.80**	**7.20**
Acetate	N (Zn^{2+}:Enz)	1.0 (± 0.2)	1.2 (±0.2)				
(ΔH_{ion} = 0.49 kJ mol^{-1})	ΔH^o_{obs}(kJ mol^{-1})	45 (±2)	35 (±2)				
MES	N (Zn^{2+}:Enz)	1.2(± 0.1)	1.3 (± 0.1)	1.7 (± 0.2)	1.8 (± 0.2)	2.0 (± 0.2)	
(ΔH_{ion} =15.53 kJ mol^{-1})	ΔH^o_{obs} (kJ mol^{-1})	17 (±1)	13 (±1)	7 (±1)	12 (±1)	11 (±2)	
Cacodylate	N (Zn^{2+}:Enz)	1.1 (± 0.2)	1.4 (± 0.2)	1.5 (± 0.2)	2.0 (± 0.2)	2.1 (± 0.2)	
(ΔH_{ion} = -1.96 kJ mol^{-1})	ΔH^o_{obs} (kJ mol^{-1})	55 (±2)	41 (±2)	41 (±2)	42 (±2)	50 (±3)	
PIPES	N (Zn^{2+}:Enz)			1.6 (± 0.2)	1.9 (± 0.2)	1.8 (± 0.2)	1.7 (± 0.3)
(ΔH_{ion}=11.45 kJ mol^{-1})	ΔH^o_{obs} (kJ mol^{-1})			17 (±3)	20 (±2)	11 (±1)	6 (±1)
MOPS	N (Zn^{2+}:Enz)					1.9 (± 0.2)	1.8 (± 0.2)
(ΔH_{ion} =21.82 kJ $mol^{-1)}$	ΔH^o_{obs} (kJ mol^{-1})					-22 (±2)	-19 (±1)
HEPES	N (Zn^{2+}:Enz)					2.1 (± 0.2)	1.9 (± 0.2)
(ΔH_{ion} =21.01 kJ mol^{-1})	ΔH^o_{obs} (kJ mol^{-1})					-16 (±1)	-22 (±2)

Enthalpies of ionisation of buffers are from Fukada, H., Takahashi., Enthalpy and heat capacity changes for the proton dissociation of various buffer components on 0.1 M potassium chloride, Struct. Funct. Genet, 1998, 33, 159-166.

SI Table 2 Summary of N and observed enthalpy change data for **cobalt** ion solution titrated into apoBcII solution as function of pH and buffer type at 25^0C.

		pH					
Buffers		**5.20**	**5.60**	**6.0**	**6.35**	**6.80**	**7.20**
Acetate (ΔH_{ion} = 0.49 kJ mol^{-1})	N (Co^{2+}:Enz) ΔH^o_{obs}(kJ mol^{-1})	0.9 (± 0.1) 20.3 (± 3)	1.0 (± 0.2) 25.5 (± 2)				
MES (ΔH_{ion} = 15.53 kJ mol^{-1})	N (Co^{2+}:Enz) ΔH^o_{obs} (kJ mol^{-1})	0.9 (± 0.1) 13.0 (± 3)	1.3 (± 0.3) 19.0 (± 2)	1.2 (± 0.2) 24.0 (± 2)	1.6 (± 0.3) 14.3 (± 2)	1.8 (± 0.2) 10.8 (± 2)	
Cacodylate (ΔH_{ion} = -1.96 kJ mol^{-1})	N (Co^{2+}:Enz) ΔH^o_{obs} (kJ mol^{-1})	0.8 (± 0.2) 39.7 (± 2)	0.9 (± 0.2) 52.7 (±2)	1.3 (± 0.2) 60.2 (± 3)	1.9 (± 0.2) 62.5 (± 3)	2.1 (± 0.2) 54.6 (± 2)	
PIPES (ΔH_{ion} = 11.45 kJ mol^{-1})	N (Co^{2+}:Enz) ΔH^o_{obs} (kJ mol^{-1})			1.3 (± 0.2) 50.2 (± 3)	1.7 (± 0.3) 12.6 (± 2)	2.0 (± 0.2) 8.0 (± 1)	2.0 (± 0.1) 7.5 (± 1)
MOPS (ΔH_{ion} = 21.82 kJ mol^{-1})	N (Co^{2+}:Enz) ΔH^o_{obs} (kJ mol^{-1})					1.8 (± 0.3) -16.1 (± 2)	1.8 (± 0.2) -16.1 (± 1)
HEPES (ΔH_{ion} = 21.01 kJ mol^{-1})	N (Co^{2+}:Enz) ΔH^o_{obs} (kJ mol^{-1})					2.2 (± 0.2) -22.3 (± 1)	1.9 (± 0.2) -24.3 (± 2)

SI Table 3 Summary of N and observed enthalpy change data for **cadmium** ion solution titrated into apoBcII solution as function of pH and buffer type at 25^0C.

		pH								
Buffers		**5.20**	**5.60**	**6.0**	**6.35**		**6.80**		**7.20**	
MES (ΔH_{ion} = 15.53 kJ mol^{-1})	N (Cd^{2+}:Enz) ΔH^o_{obs}(kJ mol^{-1})	0.9 (±0.2) 66.1 (±2)	1.0 (± 0.2) 55.2 (±3)	1.0 (± 0.2) -13.0 (±1)	0.8 (± 0.2) -19.1 (±2)	1.1 (± 0.2) -15.5 (±1)	1.0 (± 0.2) -19.1 (±1)	1.0 (± 0.2) -14.3 (±1)		
Cacodylate (ΔH_{ion} = -1.96 kJ mol^{-1})	N (Cd^{2+}:Enz) ΔH^o_{obs} (kJ mol^{-1})	1.1 (± 0.2) 50.3 (±2)	1.1 (± 0.2) 38.9 (±2)	0.9 (± 0.2) -47.9 (±2)	0.9 (± 0.2) -52.4 (±2)	1.0 (± 0.3) -17.8 (±2)	0.9 (± 0.2) -54.2 (±2)	0.9 (± 0.2) -19.0 (±2)		
PIPES (ΔH_{ion} = 11.45 kJ mol^{-1})	N (Cd^{2+}:Enz) ΔH^o_{obs} (kJ mol^{-1})				1.1(± 0.2) -36.8 (±2)	1.0 (± 0.2) -13.6 (±1)	1.0 (± 0.2) -38.9 (±3)	1.2 (± 0.3) -18.9 (±1)	1.1 (± 0.2) -42.1 (±2)	1.1 (±0.2) -15.0 (±1)
HEPES (ΔH_{ion} = 21.01 kJ mol^{-1})	N (Cd^{2+}:Enz) ΔH^o_{obs} (kJ mol^{-1})								1.0 (± 0.2) -52.0 (±2)	0.9 (± 0.2) -19.1 (±1)
MOPS (ΔH_{ion} = 21.82 kJ mol^{-1})	N (Cd^{2+}:Enz) ΔH^o_{obs} (kJ mol^{-1})								0.9 (± 0.2) -53.9 (±2)	1.1 (± 0.2) -17.0 (±1)